

# Dispersive resonance bands within the space-charge layer of a metal-semiconductor junction

S.-J. Tang,<sup>1,2,\*</sup> Tay-Rong Chang,<sup>1</sup> Chien-Chung Huang,<sup>1</sup> Chang-Yeh Lee,<sup>2</sup> Cheng-Maw Cheng,<sup>2</sup> Ku-Ding Tsuei,<sup>2,1</sup> H.-T. Jeng,<sup>3,1,†</sup> and Chung-Yu Mou<sup>1,4,‡</sup>

<sup>1</sup>Department of Physics, National Tsing Hua University, Hsinchu 30013, Taiwan

<sup>2</sup>National Synchrotron Radiation Research Center, Hsinchu 30076, Taiwan

<sup>3</sup>Institute of Physics, Academia Sinica, Nankang, Taipei 11529, Taiwan

<sup>4</sup>Physics Division, National Center for Theoretical Sciences, P.O. Box 2-131, Hsinchu, Taiwan

(Received 9 October 2009; revised manuscript received 11 February 2010; published 2 June 2010)

Based on measurements of angle-resolved photoemission, we report that in the Pb/Ge(111)- $\sqrt{3} \times \sqrt{3}$  R30° structure, in addition to three bands resembling Ge heavy hole (HH), light hole (LH), and split off (SO) bulk band edges, a fourth dispersive band resembling the nonsplit off (NSO) band is found near the surface zone center. While three Ge bulklike bands get distorted due to strong coupling between Pb and Ge, the NSO-like band gets weaker and disappears for larger thickness of Pb, which, when combined with *ab initio* calculations, indicates its localized nature within space-charge layer. Our results are clearly important for designing electronics involved with metal-semiconductor contacts.

DOI: 10.1103/PhysRevB.81.245406

PACS number(s): 73.20.At, 73.21.Fg, 79.60.Dp

The metal-semiconductor contacts are crucial in every semiconductor device since they provide communication of the device to the outside world. Depending on interface characteristics, the metal-semiconductor contacts may cause different current-voltage behavior.<sup>1</sup> One of the key factors that determine the interface characteristics is the electronic structure at the interface. It is therefore of importance to examine the electronic structure at the interface.

It is known that even a few metal atoms adsorbed on semiconductor surface can induce surface superstructures or reconstructions. The reconstruction of interface may modify the band bending at the interface,<sup>2</sup> induce a two-dimensional (2D) phase transition<sup>3</sup> or change the properties of overlayer films on top.<sup>4</sup> Another way to change the electronic structure of the interface is to dope the semiconductor. For an *n*-type semiconductor surface with surface states, if the surface state is acceptor type, space-charge effect would cause an upward band bending of the bands near the surface. It thus allows the surface-state band to cross the Fermi level so that the bulk donor states would be lifted above the Fermi level. As a result, a positive space-charge layer—the depletion layer is built up within a certain depth near the surface. In this case, the density distribution of space charge,  $\rho_{sc}$ , is related to the curvature of the band bending via the Poisson's equation. For a substantial band bending, the space-charge density,  $\rho_{sc}$ , can be approximated by a step function with  $\rho_{sc}(z) = eN_D^+ \approx eN_D = eN_{ss}/d$ , where  $N_D$  is the density of bulk donor,  $N_{ss}$  is the density of the surface states, and  $d$  is the depth of the depletion layer. The solution to the Poisson's equation with such approximation leads to the magnitude of band bending  $V_s$  at the surface<sup>5,6</sup> given by

$$|V_s| = \frac{eN_D d^2}{2\epsilon\epsilon_0}. \quad (1)$$

Therefore, roughly  $d^2 \propto 1/N_D$  so the band bending slope or potential gradient would be much higher for the highly doped semiconductor. Figures 1(a) and 1(b) show the comparison of such a behavior for highly doped and lightly

doped *n*-type semiconductors, respectively. For the case of the former, the depletion layer is called the inversion layer due to the fact the charge density of holes turns to exceed that of free electrons at the depth near surface. For the highly doped semiconductor, the surface-state density or bandwidth, as shown by the length of the shaded rectangular in Fig. 1(a), could slightly increase with increasing doping density as a result of the fact that donor electrons in the conduction band reduce their energies by occupying the acceptorlike surface states. Consequently, the higher upward band bending of the valence-band maximum and the increment of surface-state bandwidth would cause overlap between the valence-band maximum and the surface state in ( $E, k$ ) space, hence causing the strong interaction between them.

Experimentally, direct determination of electronic dispersion at the interface has been lacking until in 2005, Takeda *et al.* first measured quantum-well states (QWSs) for the *n*-type

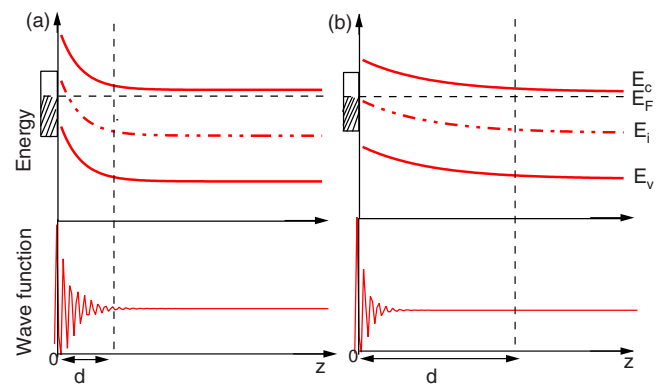


FIG. 1. (Color online) The energy positions of valence-band maximum ( $E_v$ ), conduction-band minimum ( $E_c$ ), intrinsic energy ( $E_i$ ), and Fermi level ( $E_f$ ) as a function of the distance  $z$  from the surface of the (a) highly doped and (b) lightly doped *n*-type semiconductor. The bandwidth of occupied (unoccupied) acceptor-type surface state is represented by a shaded (blank) rectangular. The bottom panel shows the wave function of the acceptor-type surface state corresponding to (a) and (b).

Si quantum well within the In/Si(111)- $\sqrt{7} \times \sqrt{3}$  surface structure by angle-resolved photoemission.<sup>7</sup> The in-plane dispersions of the hole subbands in a highly doped semiconductor was first observed. Later, Nathan *et al.*<sup>8</sup> further discovered fine-structured electronic fringes near the silicon valence-band edge in atomically uniform Ag films grown on highly doped *n*-type Si(111). These fringes were attributed to the quantum slope potential in the inversion layer. Nevertheless, to date, there has been no experimental observation of the signature as a result of large overlap between surface states and the valence-band maximum at the surface or interface, as the case shown in Fig. 1(a).

In this paper, based on measurements of angle-resolved photoemission, we use highly doped *n*-type Ge(111) wafer and investigate the interface electronic structure for the Pb/Ge(111)- $\sqrt{3} \times \sqrt{3}$   $R30^\circ$  structure. In addition to three bands resembling Ge bulk band edges, a fourth dispersive band resembling the nonsplit off (NSO) band is found near the surface zone center. The evolution of these four bands with increasing thickness of Pb films at 2, 4, and 6 ML was also examined. By further comparison with first-principles calculations, we show that the largest weight of the NSO-like band is located near the interface of Pb and Ge, confirming the localized nature of NSO-like band.

In our study, angle-resolved photoemission measurements were performed by Scienta R3000 energy analyzer with a He I UV light of photon energy 21.2 eV. Some additional data were taken by the 21B1-U9 beamline in the National Synchrotron Radiation Research Center in Taiwan; the results were consistent. The highly doped *n*-type Ge(111) wafer,  $\sim 10^{18}$  (1/cm<sup>3</sup>), was used. The clean procedure for a Ge(111)- $c(2 \times 8)$  surface was described elsewhere.<sup>9</sup> For the formation of Pb/Ge(111)- $\sqrt{3} \times \sqrt{3}$   $R30^\circ$  structure,  $\sim 3$  ML of the Pb film was deposited and the substrate was subsequently annealed from RT to 400 °C. The Pb/Ge(111)- $\sqrt{3} \times \sqrt{3}$   $R30^\circ$  structure thus obtained is  $\beta$  phase as there was no phase transition<sup>10</sup> observed when it was cooled down to -150 °C for photoemission measurement. Overlayer uniform Pb film was formed by depositing Pb onto the Pb/Ge(111)- $\sqrt{3} \times \sqrt{3}$   $R30^\circ$  structure kept at -150 °C. The calibration of film thickness was done by monitoring the intensity and energy positions of Pb QWS peak at normal emission as a function of deposition time.<sup>11</sup>

To unravel nature of the observed electronic structures, we also perform the first-principles calculations. Our calculations were carried out using the highly accurate full-projected augmented wave method<sup>12</sup> as implemented in the VASP package<sup>13</sup> based on the local-density approximation. The lattice structure of bulk Ge was optimized using a  $13 \times 13 \times 7$  Monkhorst-Pack *k*-point mesh over the Brillouin zone with cutoff energy of 500 eV. The Ge(111)- $1 \times 1$  unreconstructed surface was simulated by a 36-layer Ge slab (thickness of  $\sim 60$  Å) with a vacuum thickness larger than 10 Å, well separating the slabs. The self-consistent calculations were performed over 21 *k*-point mesh over the two-dimensional irreducible Brillouin zone using 27 266 plane waves with a cutoff energy of 500 eV under geometry optimization. The long-layer terminated surface was employed to simulate the case under study in which Pb atoms are believed to mix with the Ge atoms of the top short layer. Based on the

optimized structure, the spin-orbital coupling was included in the band-structure calculations both for the bulk and surface.

In Fig. 2, we show the grayscale representations of the photoemission results for the clean Ge(111)- $c(2 \times 8)$  surface (top), and Pb/Ge(111)- $\sqrt{3} \times \sqrt{3}$   $R30^\circ$  surface (bottom), respectively, in two symmetry directions. Note that symbols on the top of the Fig. 2 represent the symmetry points for  $(1 \times 1)$  surface Brillouin zone while symbols at the bottom represent the symmetry points for  $\sqrt{3} \times \sqrt{3}$   $R30^\circ$  surface Brillouin zone. It is clear that in the photoemission results either for Ge(111)- $c(2 \times 8)$  or for Pb/Ge(111)- $\sqrt{3} \times \sqrt{3}$   $R30^\circ$ , dispersive energy bands are observed about the symmetry points corresponding to the surface zone boundaries, as indicated by vertical bars. These bands are likely to originate from the surface structures. Even though it is still of interest to investigate in detail those surface electronic bands for both surfaces, and compared them with previously measured and calculated results,<sup>10,14-18</sup> the focus of this paper, nevertheless, is on the change in energy-band dispersions about the surface zone center  $\bar{\Gamma}$  from Ge(111)- $c(2 \times 8)$  to Pb/Ge(111)- $\sqrt{3} \times \sqrt{3}$   $R30^\circ$ . Clearly, Fig. 2 shows a set of four new bands near the surface zone center in both symmetry directions in the Pb/Ge(111)- $\sqrt{3} \times \sqrt{3}$   $R30^\circ$  surface. These four new bands have neither correspondence to the energy bands in Ge(111) surface nor the energy bands in Pb/Ge(111)- $\sqrt{3} \times \sqrt{3}$   $R30^\circ$ , measured or calculated previously.<sup>10,14-18</sup> However, at the first sight, those bands resemble the bulk hole band edges of Ge. Since the Ge(111) used in this experiment is highly doped *n* type, the four new bands observed might be related to the doping effect from Ge(111). In Figs. 3(a) and 3(b), we superimposed the calculated Ge bulk band edges dispersing in the same symmetry direction ( $\Gamma K$  for bulk,  $\bar{\Gamma}\bar{K}$  for  $1 \times 1$ , and  $\bar{\Gamma}\bar{M}\bar{K}$  for  $\sqrt{3} \times \sqrt{3}$   $R30^\circ$ ) onto the 2D image data. As is evident, the calculated bulk band edges, HH, LH, SO (dashed curves), and NSO (dot curves), match the measured four bands very well within the large energy range from Fermi level down to 1.0 eV. The photon-energy-dependent data, which is not presented in this paper, shows the energies of the four bands do not shift with photon energies, indicating the surface related nature. Hence, the scenario represented by Fig. 1(a) seems to apply in which surface state become a surface resonance (SR), crossing the inversion layer and strongly mixing with bulk band edges. Similar results were observed by Tang *et al.*<sup>19</sup> that the surface state of Ag thin film at the thickness smaller than its decay length exhibits the energy dispersions resembling HH, LH, and SO band edges as a result of the strong interaction with Ge bulk edges.

However, two questions still remain. First, why are not those four bands observed from a clean highly doped *n*-type Ge(111) surface? Second, why does the NSO-like band exist, which does not have the counterpart in the bulk? The surface-state bands of clean Ge(111)- $c(2 \times 8)$  about the zone center, as recently reexamined by Razado-Colambo *et al.*,<sup>16</sup> mostly originated from the dangling bonds of rest atoms and adatoms, or back bonds few layers below them near the surface,<sup>14-16</sup> which are intimately related to the  $c(2 \times 8)$  surface reconstruction. The higher intensities of those localized

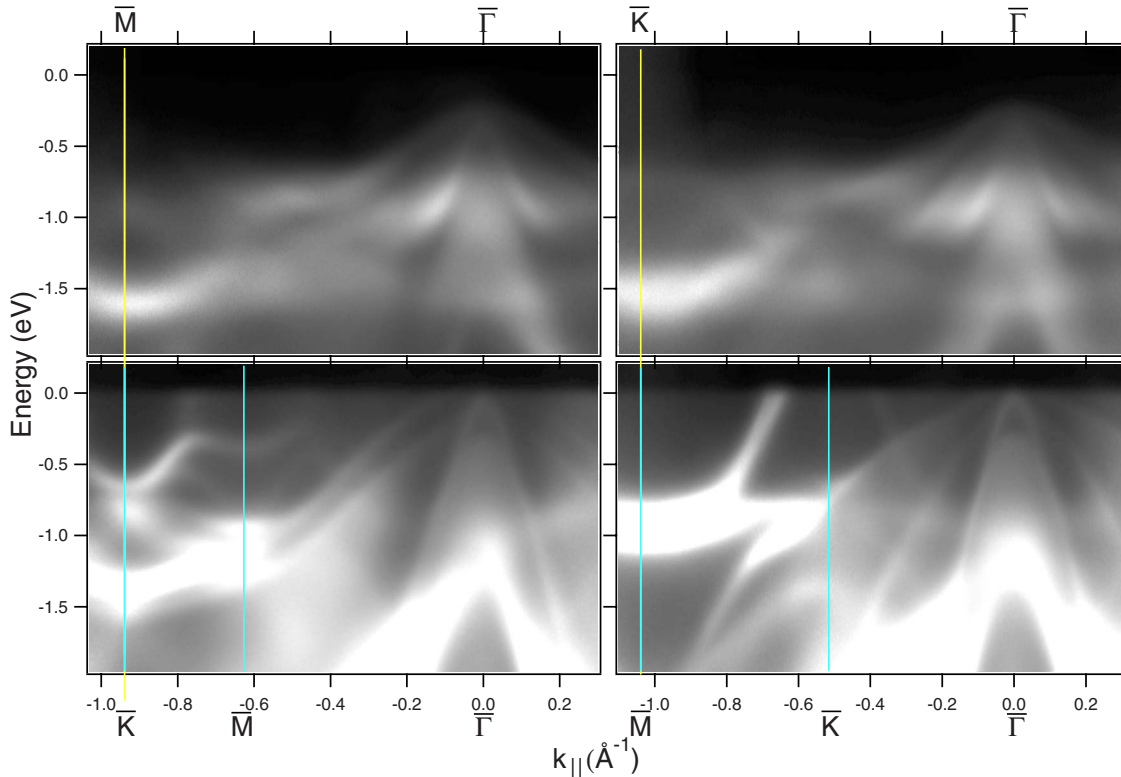


FIG. 2. (Color online) Angle-resolved photoemission data presented as grayscale images as a function of energy and  $k_{\parallel}$  for the clean Ge(111)- $c(2 \times 8)$  surface (top), and Pb/Ge(111)- $\sqrt{3} \times \sqrt{3}$   $R30^\circ$  surface (bottom), respectively, in two symmetry directions.

surface-state bands would cover the relatively lower intensities of the four bands.<sup>20</sup> In addition, adsorption of Pb on Ge(111) change the surface reconstruction from  $c(2 \times 8)$  to  $\sqrt{3} \times \sqrt{3}$   $R30^\circ$ , hence diminishing these Ge(111)- $c(2 \times 8)$  localized surface-state bands and facilitating the appearance of the four bands. Figure 3(b) shows the energy-band dispersions for 2 ML Pb on Ge(111) and surprisingly, the four bands remain and three bands, corresponding to HH, LH, and SO, get even sharper and more intense. The independence of these three bands on the lattice structures above the Ge(111) surface confirms that their wave functions have most of amplitudes below the surface area, going through the inversion layer, as depicted by the bottom of Fig. 1(a). This interesting finding from 2 ML yet points to another role Pb plays, which is to increase the SR density or bandwidth so as to have stronger interaction with Ge bulk band edges even though the SR were originally contributed by the bulk donors in the inversion layer. When Pb film get thicker, the coupling of Ge bulk band edges with SR should transit to the coupling with the quantum-well resonances (QWRs) of Pb films, and 2 ML is at the intermediate position for this transition. As seen from Figs. 3(c), 3(d), 3(g), and 3(h), the curvatures of three bands corresponding to HH, LH, and SO band edges get expanded but the fourth band corresponding to NSO yet get weaker and tend to disappear with increasing thickness from 4 to 6 ML.<sup>21</sup> The density of states for Pb electrons are not dominated by Ge bulk edges any more; instead, the three new bands can be simulated through the Anderson's interaction between discrete QWR and continuous bulk edges.<sup>9</sup> The net effect is like that the Ge band edges split the QWR bands

into several segments. For comparison, the expected subbands of QWS for free-standing Pb films of 2, 4, and 6 ML, based on a tight-binding calculation of the bulk band structure of Pb (Ref. 22) are superimposed on to the data, as shown by the solid curves in Fig. 3(f)–3(h). The crossover of the QWR band and Ge band edges presents kink or break like structures, which are more evident for 6 ML.

Due to the observed fact that the intensity of the NSO-like band get weaker and tend to disappear with increasing thickness, the origin of the fourth band should not be due to the coupling between the thin film and substrate, and hence not be related to the valence-band bending. The mean-free path of the electrons corresponding to the photon energy used (21.2 eV) is about 10 Å, which is about 4 ML of Pb film, wherein the intensity of the fourth band was observed to start decaying. Therefore, it is reasonable to consider it as some unique 2D band, which is inherently localized within the space-charge layer. To simulate the hole subband dispersion of the space-charge layer, we perform first-principles calculation based on a 36-layer Ge(111) slab.<sup>23</sup> The spectrum is shown in Fig. 4. It is clearly seen that in Fig. 4(a), there is a trace of a SR-type band isotropically across the discrete hole subbands in the directions from the surface zone center  $\bar{\Gamma}$  to the two surface zone boundaries at  $\bar{K}$  and  $\bar{M}$ , respectively. The trace of the band is extracted as indicated by the blue circles inside the rectangular frame of the Fig. 4(b), and superimposed it onto our 2D photoemission image data for 2 ML of Pb film in both symmetry directions within the same range as the rectangular frame. As seen in Fig. 4(c), this calculated SR band matches the fourth band very well, lo-

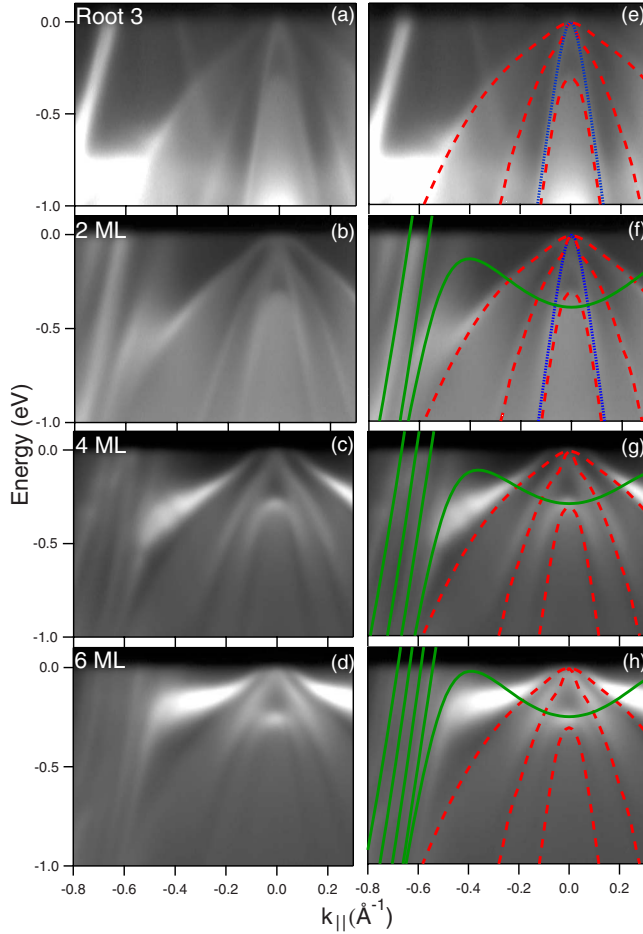


FIG. 3. (Color online) Angle-resolved photoemission data presented as grayscale images as a function of energy and  $k_{||}$  for (a) Pb/Ge(111)- $\sqrt{3} \times \sqrt{3}$   $R30^\circ$ , and (b) 2 ML (c) 4 ML and (d) 6 ML of Pb on Ge(111) in the symmetry direction  $\Gamma\bar{K}$  for bulk,  $\Gamma\bar{M}\bar{K}$  for  $\sqrt{3} \times \sqrt{3}$   $R30^\circ$ , and  $\Gamma\bar{K}$  for  $1 \times 1$ . The calculated bulk HH, LH, SO (dashed curves), and NSO (dot curves) bands of Ge, and the calculated QWS subbands (solid curves) of Pb films are superimposed onto the data in (e), (f), (g), and (h), correspondingly.

cated inside the gap induced by the spin-orbital splitting (SOS) of the three-hole band edges. According to our calculation, this SR band has the mixture of  $p_x$  and  $p_y$  symmetry. Figure 4(d) shows the  $z$  profile of the charge density of this SR at  $\bar{\Gamma}$ . As seen, it has negligible electron density at and above the first layer; instead, 47% and 39% of the electron density are distributed over the second and third layer, and over the fourth and fifth layer, respectively. This result explains why the fourth band whereas a Ge inherent 2D band, is still observed after Pb deposition because of its delocalization from the surface. Surface states existing within the SOS-induced gap have been previously observed on the metal surfaces.<sup>24–26</sup> The existence of such kind of surface state is very likely for Ge surface since Ge has fairly large SOS-induced gap of  $\sim 0.3$  eV at the zone center. Nevertheless, this gap is a pseudogap in light of the fact that the hole subbands still exist inside the gap and therefore, the fourth band observed is actually a SR.

In conclusion, we have studied electronic structures of Pb

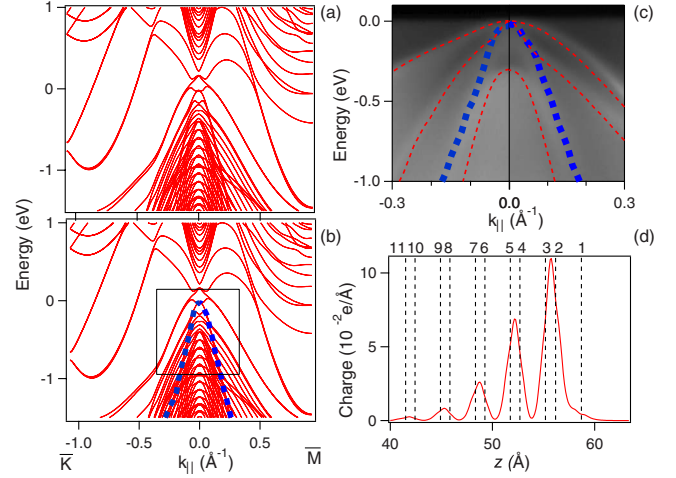


FIG. 4. (Color online) (a) The hole subband dispersions of Ge(111) space-charge layer in the symmetry directions  $\bar{\Gamma}\bar{K}$  and  $\bar{\Gamma}\bar{M}$ , based on a 36-layer slab model. (b) The trace of SR band, as indicated by the blue circles, extracted from the hole subband dispersions in both symmetry directions. (c) The extracted SR band superimposed on the angle-resolved photoemission data for 2 ML Pb on Ge(111) in both symmetry directions. The red dashed curves are the corresponding calculated HH, LH, and SO hole band edges. (d) The charge density  $z$  profile for the SR state at  $\bar{\Gamma}$ . The layer numbers are indicated on the top.

thin films on highly doped  $n$ -type Ge(111) surface. Due to the largely reduced depth of the inversion layer, there is a strong electron-electron coupling between the Pb thin film and the Ge hole band edges within the layer. With increasing thickness of Pb film, this coupling changes from the type of SR-bulk edge coupling to the type of QWR-bulk edge coupling. The NSO-like band observed from the very thin film is another type of SR band derived from the SOS-induced gap. The agreeable match between the measurement and first-principles calculation without assuming the shape of the space-charge layer indicates that this NSO band is an intrinsic SR state localized within the space-charge layer of Ge(111) surface, regardless of the doping concentration of Ge. However, more delicate and detailed calculation work is indeed needed in the future in order to fully understand the origin of the NSO band. We believe this recently found SR band is very important to the property of semiconductor interface or surface such as the electric conductivity, which has been studied experimentally and theoretically<sup>27,28</sup> mainly from the Si surface that, however, has very negligible SOS induced gap. In addition to that the spin transport induced by the Rashba splitting at the interface of the semiconductor has gained massive interest recently.<sup>29</sup> Therefore, the influence of this SR band on the properties of Ge(111) surface and interface, and its potential application is yet to uncover.

The research is supported by the National Science Council of Taiwan (Grants No. NSC 98-2112-M-007-017-MY3 and No. NSC 95-2112-M-007-062-MY3) and by the National Synchrotron Radiation Research Center. The author would like to thank B.-S. Fang for providing the vacuum chamber and instruments in setting up the angle-resolved photoemission system.

\*sjtang@phys.nthu.edu.tw

†jeng@phys.sinica.edu.tw

‡mou@phys.nthu.edu.tw

- <sup>1</sup>E. H. Rhoderick and R. H. Williams, *Metal-Semiconductor Contacts* (Clarendon Press, Oxford, 1998).
- <sup>2</sup>J. A. Carlisle, T. Miller, and T.-C. Chiang, *Phys. Rev. B* **45**, 3400 (1992).
- <sup>3</sup>J. M. Carpinelli, H. H. Weitering, E. W. Plummer, and R. Stumpf, *Nature (London)* **381**, 398 (1996).
- <sup>4</sup>D. A. Ricci, T. Miller, and T.-C. Chiang, *Phys. Rev. Lett.* **95**, 266101 (2005).
- <sup>5</sup>H. Lüth, *Surfaces and Interfaces of Solid Materials*, 3rd ed. (Springer-Verlag, Berlin, 1998).
- <sup>6</sup>W. Mönch, *Semiconductor Surfaces and Interfaces* (Springer, Berlin, 1995).
- <sup>7</sup>S. N. Takeda, N. Higashi, and H. Daimon, *Phys. Rev. Lett.* **94**, 037401 (2005).
- <sup>8</sup>N. J. Speer, S.-J. Tang, T. Miller, and T.-C. Chiang, *Science* **314**, 804 (2006).
- <sup>9</sup>S.-J. Tang, L. Basile, T. Miller, and T.-C. Chiang, *Phys. Rev. Lett.* **93**, 216804 (2004).
- <sup>10</sup>H. Morikawa, I. Matsuda, and S. Hasegawa, *Phys. Rev. B* **77**, 193310 (2008).
- <sup>11</sup>M. H. Upton, T. Miller, and T.-C. Chiang, *Appl. Phys. Lett.* **85**, 1235 (2004).
- <sup>12</sup>P. E. Blöchl, *Phys. Rev. B* **50**, 17953 (1994); G. Kresse and D. Joubert, *ibid.* **59**, 1758 (1999).
- <sup>13</sup>G. Kresse and J. Hafner, *Phys. Rev. B* **48**, 13115 (1993); G. Kresse and J. Furthmüller, *Comput. Mater. Sci.* **6**, 15 (1996); *Phys. Rev. B* **54**, 11169 (1996).
- <sup>14</sup>J. Aarts, A. J. Hoeven, and P. K. Larsen, *Phys. Rev. B* **37**, 8190 (1988).
- <sup>15</sup>R. D. Bringans, R. I. G. Uhrberg, and R. Z. Bachrach, *Phys. Rev. B* **34**, 2373 (1986).
- <sup>16</sup>I. Rizado-Colambo, J. He, H. M. Zhang, G. V. Hansson, and R. I. G. Uhrberg, *Phys. Rev. B* **79**, 205410 (2009).
- <sup>17</sup>A. Mascaraque, J. Avila, E. G. Michel, and M. C. Asensio, *Phys. Rev. B* **57**, 14758 (1998).
- <sup>18</sup>J. A. Carlisle, T. Miller, and T.-C. Chiang, *Phys. Rev. B* **47**, 10342 (1993).
- <sup>19</sup>S.-J. Tang, T. Miller, and T.-C. Chiang, *Phys. Rev. Lett.* **96**, 036802 (2006).
- <sup>20</sup>The intensity of 2D image of photoemission spectra for Pb/Ge(111)- $\sqrt{3} \times \sqrt{3}$  R30° in Fig. 1 was intentionally enhanced. The intensities of four bands are actually weak.
- <sup>21</sup>Due to special ratio of  $k_F$  and layer spacing for Pb(111) film, the QWR gets close to Fermi level and interact with Ge valence-band maximum every two layers. Therefore the data of 1, 3, and 5 ML are not shown, wherein the QWR are relatively far from Fermi level and more free-electronlike.
- <sup>22</sup>D. A. Papconstantopolous, *Handbook of the Band Structure of Elemental Solids* (Plenum Press, New York, 1986).
- <sup>23</sup>According to Eq. (1), with the dielectric constant ( $\epsilon=16$ ) for Ge and the magnitude of band bending  $V_s \sim 0.17$  eV (the difference between valence maximum positions of highly doped and undoped Ge), the thickness of space-charge layer for  $n$ -type highly doped,  $\sim 10^{18}$  (1/cm<sup>3</sup>), Ge(111) surface is estimated to be 388 Å, corresponding to  $\sim 210$  layers. Even though we only used a 36-layer slab model to approximate the subbands of space-charge layer, the surface resonance feature extracted, which resembles NSO band is still valid. A 108-layer slab model was ever used and the result is similar.
- <sup>24</sup>R. H. Gaylord and S. D. Kevan, *Phys. Rev. B* **36**, 9337 (1987).
- <sup>25</sup>P. L. Wincott, N. B. Brookes, D. S. Law, and G. Thornton, *Phys. Rev. B* **33**, 4373 (1986).
- <sup>26</sup>B.-S. Fang, W.-S. Lo, and H.-H. Chen, *Phys. Rev. B* **47**, 10671 (1993).
- <sup>27</sup>T. Tanikawa, K. Yoo, I. Matsuda, and S. Hasegawa, *Phys. Rev. B* **68**, 113303 (2003).
- <sup>28</sup>J. W. Wells, J. F. Kallehauge, T. M. Hansen, and Ph. Hofmann, *Phys. Rev. Lett.* **97**, 206803 (2006).
- <sup>29</sup>T. Matsuyama, R. Kürsten, C. Meißner, and U. Merkt, *Phys. Rev. B* **61**, 15588 (2000).